OPTIMAL SLIDING MODE CONTROL FOR SEISMIC CONTROL OF BUILDINGS EQUIPPED WITH ATMD

M. Khatibinia[*, †,1], M. Mahmoudi[2] and H. Eliasi[3]
[1]Department of Civil Engineering, University of Birjand, Birjand, Iran
[2]Department of Civil Engineering, Khayyam University, Mashhad, Iran
[3]Department of Electrical Engineering, University of Birjand, Birjand, Iran

ABSTRACT

Active tuned mass damper (ATMD) systems have attracted the considerable attention of researchers for protecting buildings subjected to earthquake loading. This paper presents the development of an optimal sliding mode control (OSMC) system for a building equipped with ATMD. In the OSMC technique, a linear sliding surface is used with the slope of this surface designed such that a given (or desired) cost function is minimized. The design is obtained by transforming the system into the regular form. In the regular form, the system is divided into two subsystems inclding: a control term explicitly appears, and other control terms do not appear. In order to demonstrate the capability of the OSMC system, an 11–story realistic building with a TMD installed on the top story of the structure is considered. For achieving this purpose, four well–known earthquake records are selected to evaluate the performance of the OSMC system. Results show that the OSMC technique performs better than other control techniques in the reduction of seismic responses of the structure.

1. INTRODUCTION

The efficiency of active, hybrid and passive control methods for the control of civil engineering structures have been demonstrated in order to protect them subjected to environmental loads (i.e., wind and earthquake) [1, 2]. The main aim of the control systems is to reduce the structural responses, damages and demands.

---

[*]Corresponding author: Department of Civil Engineering, University of Birjand, Birjand, Iran
[†]E-mail address: m.khatibinia@birjand.ac.ir (M. Khatibinia)

Tuned mass dampers (TMDs) as the oldest passive seismic control devices are tuned with a vibration frequency close to the fundamental frequency of structures. The TMD system consists of a mass, spring, and a viscous damper attached to a vibrating main system in order to attenuate any undesirable vibrations. Due to the uncertainty in determining the parameters of structure (i.e. its mass and stiffness), accurately assigning the natural frequency of the structure is not possible. Therefore, the efficient performance of the TMD system is attenuated and their application is limited in a narrow range of load frequencies [3]. In order to overcome these shortcomings, active TMDs (ATMDs) have been proposed [4 , 5].

In a structure equipped with an ATMD, an actuator installed between the structure and the TMD system applies a control force in real time to the ATMD and its reaction is applied to the structure. The selection of a suitable control scheme for tuning the control force has been considered as a key role in the successful application of an ATMD system. By selecting an effective control scheme, a suitable trade–off can be also provided between two conflicting objective of reducing control force and reducing structural responses. The most common control methods for this case are linear quadratic regulator (LQR) [2], linear quadratic Gaussian (LQG) [6, 7], H_2 and H_∞ [8–10], fuzzy logic controller (FLC) [11–14], and PID controller [15–17].

The sliding mode control (SMC) technique as a nonlinear method was introduced for the active control of civil structures by Yang et al. [18] and Adhikari and Yamaguchi [19], and is based on high–frequency switching. Because of the variable structure of the SMC technique, it has the capable of switching between different control laws. Since SMC is not sensitive against changes and external excitation, the selection of the method in comparison with other control techniques has been considered as the best scheme [20].

This paper deals with the development of an optimal sliding mode control (OSMC) system for a building equipped with ATMD. In this technique, a linear sliding surface, which passes through the origin, is used with the slope of this surface designed such that a given (or desired) cost function is minimized. The design is started by transforming the system into the regular form. In the regular form, the system is divided into two subsystems including: (1) a control term explicitly appears, and (2) other control terms do not appear. In order to prove the validity of OSMC, an 11–story realistic building with a TMD installed on the top floor of the structure is considered. For this end, four well–known earthquake records are adopted to evaluate the performance of OSMC. The simulation results show that the OSMC technique performs better than LQR, PID controllers in reduction of seismic responses of the structure.

2. EQUATIONS OF MOTION

2.1 Structure equipped with a TMD

An *N*–degree–of–freedom linear structure equipped with a TMD, installed on the top floor, subjected to excitation acceleration, $\ddot{x}_g(t)$, is considered. The equation of motion of the structure can be written as:

$$\mathbf{M}\ddot{x}(t) + \mathbf{C}\dot{x}(t) + \mathbf{K}x(t) = -\mathbf{M}\,\mathbf{r}\,\ddot{x}_g(t) \tag{1}$$

where $\mathbf{M}$, $\mathbf{C}$, $\mathbf{K}$ and x are the mass, damping, and stiffness matrices and the displacement vector with the below formulations:

$$x(t) = \{x_1 \quad x_2 \quad \cdots \quad x_N \quad x_d\}^T \tag{2}$$

$$\mathbf{M} = diag(m_1 \ m_2 \cdots m_N \ m_d) \tag{3}$$

$$\mathbf{K} = \begin{bmatrix} (k_1 + k_2) & -k_2 & & & & \\ -k_2 & (k_2 + k_3) & -k_3 & & 0 & \\ & . & . & & & \\ & & . & . & . & \\ & & & . & . & . \\ & sym & & -k_N & (k_N + k_d) & -k_d \\ & & & & -k_d & k_d \end{bmatrix} \tag{4}$$

In addtition, k_d and m_d are the stiffness coefficient and the mass of TMD. r is the $(N+1) \times 1$ vector of ones which represented the location vector of the earthquake excitation.

According to the Rayleigh damping method, the structural damping matrix $\mathbf{C}$ can be assumed to be proportional to the mass and stiffness matrices as shown in Eq. (5).

$$\mathbf{C} = \frac{2\xi\omega_1\omega_2}{\omega_1 + \omega_2}\mathbf{M} + \frac{2\xi}{\omega_1 + \omega_2}\mathbf{K} \tag{5}$$

in which ω_1 and ω_2 are the structural frequencies in first and second modes, respectively. In addition, ξ is the critical damping ratio for the first two modes.

2.2 Structure equipped with an ATMD

For a building subjected to ground excitations and equipped with an active control system, the linear equations of motion can be written in matrix form as:

$$\mathbf{M}\ddot{x}(t) + \mathbf{C}\dot{x}(t) + \mathbf{K}x(t) = -\mathbf{M}\,r\,\ddot{x}_g(t) + \mathbf{D}u(t) \tag{6}$$

where $u(t) \in R$ is the control force. Also, $\mathbf{D}$ is an $N \times 1$ location vector for the control forces. Vector $\mathbf{D}$ is defined based on the location of actuators in the structure.

In a structure equipped with an ATMD situated on the top story, an actuator, which is placed between the structure and the TMD system, applies a control force in real time to ATMD and its reaction applied to the top story of the structure. The equation of the structural system can be written in the standard state–space form as shown in Eq. (7):

$$\dot{\tilde{\mathbf{X}}}(t) = \mathbf{A}\tilde{\mathbf{X}}(t) + \mathbf{B}u(t) + \mathbf{H}\ddot{x}_g(t) = \mathbf{A}\tilde{\mathbf{X}}(t) + \mathbf{B}u(t) + \mathbf{E}(t)$$
$$y(t) = \mathbf{G}\tilde{\mathbf{X}}(t) \tag{7}$$

in which

$$\tilde{\mathbf{X}}(t) = \left\{ \begin{array}{c} \boldsymbol{x}(t) \\ \dot{\boldsymbol{x}}(t) \end{array} \right\} \tag{8}$$

In addition, the state matrix **A**, input matrix **B**, matrix **H** and output matrix **G** are given as:

$$\mathbf{A} = \begin{bmatrix} \mathbf{0} & \mathbf{I} \\ -\mathbf{M^{-1}K} & -\mathbf{M^{-1}C} \end{bmatrix} \tag{9}$$

$$\mathbf{B} = \begin{bmatrix} \mathbf{0} \\ \mathbf{M^{-1}D} \end{bmatrix} \tag{10}$$

$$\mathbf{H} = \begin{bmatrix} \mathbf{0} \\ -\mathbf{r} \end{bmatrix} \tag{11}$$

$$\mathbf{G} = \begin{bmatrix} \mathbf{I} & \mathbf{0} \end{bmatrix} \tag{12}$$

3. OPTIMAL SILIDING MODE CONTROL

3.1.An overview of SMC controller

Sliding mode control (SMC) is a robust control technique that alters the dynamics of a system by application of a discontinuous control signal. The control signal forces the system to slide along a cross–section of the system's normal behavior. Controllers–based SMC are designed to drive the system states onto a particular surface in the state space called sliding surface [21]. Once the sliding surface is reached, SMC keeps the states on the close neighborhood of the sliding surface. Hence, SMC is a two–part controller design. The first part involves the design of a sliding surface so that the sliding motion satisfies design specifications. The second part is concerned with the selection of a control law that will make the switching surface attractive to the system state. From a practical point of view, SMC can be used for controlling nonlinear processes subject to external disturbances and heavy model uncertainties.

The main advantages of SMC contain two issues. First, the dynamic behavior of a system may be tailored by the particular choice of the sliding function. Secondly, the closed loop response becomes totally insensitive to some particular uncertainties. This principle extends to model parameter uncertainties, disturbance and non–linearity [21]. The most significant factors of the SMC technique are Reaching Mode (RM), Sliding Mode (SM) and Steady State Mode (SSM). The terms have very specific meanings. Starting from the initial condition, the phase trajectory is attracted to the sliding manifold during the RM. Once the phase trajectory hits the manifold it slides towards the origin of the phase plane called SM. Then, the phase trajectory stays at the origin and steady state is achieved. The whole exercise of designing the SMC law requires a fairly good mathematical model of the system. The switching component in the SMC law is desired in most of the cases to ensure the phase trajectory does not leave the sliding manifold and thus it reaches origin. Once the trajectory

reaches to sliding phase, the system dynamics are governed by the surface dynamics and hence, the system is immune to external bounded disturbances [21].

3.2.Design of optimal SMC

In order to design the optimal SMC (OSMC), the sliding surface is defined as [21]:

$$S = \mathbf{P}\tilde{\mathbf{X}} = 0 \tag{13}$$

where $S \in R$ is the sliding variable. $\mathbf{P}$ is a $(1 \times N)$ matrix to be determined such that the motion on the sliding surface is stable.

The OSMC technique makes S equal to zero in finite time and then maintain the condition S=0 for all future time. In other words, OSMC consists of a reaching mode, during which the sliding variable moves to the sliding surface, and a sliding mode, during which the sliding variable is confined to the sliding surface and S has no variation from sliding surface in system without uncertainty. In OSMC, the control input is designed as follow [21]:

$$u = u_{reach} + u_{eq} \tag{14}$$

where u_{reach} is the reaching control law.

This part of control law is selected such that outside the surface S, the following sliding condition holds,

$$\frac{1}{2}\frac{d}{dt}S^2 \le -\gamma|S| \tag{15}$$

where γ is a positive constant. This condition forces all trajectories to slide toward the surface S.

Fig. 1 shows the reaching mode schematically. u_{eq} is an equivalent control law which can be found by setting $\dot{S} = 0$ in absence of external disturbance $\mathbf{E}(t)$ and considering Eq. (13). This control law keeps the response trajectory of system on sliding surface, once it reaches there. It follows from Eqs. (7) and (13) that

$$\dot{S} = \mathbf{P}\dot{\tilde{\mathbf{X}}} = \mathbf{P}(\mathbf{A}\tilde{\mathbf{X}} + \mathbf{B}\,u_{eq}) = 0 \tag{16}$$

The solution of Eq. (16) yields the closed from of u_{eq} as follows:

$$u_{eq} = -(\mathbf{PB})^{-1}\mathbf{PA}\tilde{\mathbf{X}} \tag{17}$$

Now, in order to satisfy sliding condition (12) despite external disturbance $\mathbf{E}(t)$, u_{reach} is considered as follows:
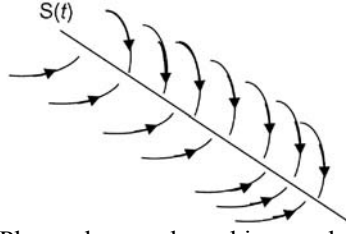
$$u_{reach} = -(\mathbf{PB})^{-1} \times k\,sgn(S) \tag{18}$$

Figure 1. Phase plane and reaching mode in OSMC

where k is a positive constant and $k > |\mathbf{E}(t)|$. $sign(\cdot)$ is the sign function. From (7), (15), (17) and (18), it is obtained as:

$$\dot{S}S = \mathbf{E}(t)S - k|S| \tag{19}$$

So that, letting $k = \gamma + sup|\mathbf{E}(t)|$ leads to satisfy sliding condition (15). One systematic approach for the determination of the matrix $\mathbf{P}$ is to use the method of LQR. This method is based on minimizing the integral of the quadratic function of the state vector as follows [21]:

$$J = \int_t^\infty \tilde{\mathbf{X}}'(\tau)\mathbf{Q}\,\tilde{\mathbf{X}}(\tau)d\tau \tag{20}$$

in which

$$\tilde{\mathbf{X}} = \begin{bmatrix} \tilde{\mathbf{X}}_1' & \tilde{X}_2' \end{bmatrix}' \quad ; \quad \mathbf{Q} = \begin{bmatrix} \mathbf{Q}_{11} & \mathbf{Q}_{12} \\ \mathbf{Q}_{21} & \mathbf{Q}_{22} \end{bmatrix} \tag{21}$$

where $\tilde{\mathbf{X}}_1' \in R^{2n-1}$ and $\tilde{X}_2' \in R$. $\mathbf{Q}_{11}$ and Q_{22} are $(2N-1)\times(2N-1)$ and 1×1 matrices, respectively.

Since the system (7) is single input and in regular form, let $\mathbf{A}$ and $\mathbf{P}$ be partitioned as follows:

$$\mathbf{A} = \begin{bmatrix} \mathbf{A}_{11} & \mathbf{A}_{12} \\ \mathbf{A}_{21} & \mathbf{A}_{22} \end{bmatrix} \quad ; \quad \mathbf{P} = \begin{bmatrix} \mathbf{P}_1 & \vdots & P_2 \end{bmatrix} \tag{22}$$

in which $\mathbf{A}_{11}, \mathbf{A}_{22}, \mathbf{P}_1$ a nd P_2 are $(2N-1)\times(2N-1)$ and 1×1 matrices, $1\times(2N-1)$ vector and scalar, respectively. Substituting (22) into (7) and (13), one can be represented the equations of motion on the sliding surface as follows:

$$\dot{\tilde{\mathbf{X}}}_1 = \mathbf{A}_{11}\tilde{\mathbf{X}}_1 + \mathbf{A}_{12}\tilde{X}_2 \tag{23}$$
$$S = \mathbf{P}_1\tilde{\mathbf{X}}_1 + P_2\tilde{X}_2 = 0 \tag{24}$$

From Eqs. (23) and (24), the following equation is obtained:

$$\dot{\tilde{\mathbf{X}}}_1 = (\mathbf{A}_{11} - \mathbf{A}_{12}\mathbf{P}_2^{-1}\mathbf{P}_1)\tilde{\mathbf{X}}_1 \tag{25}$$

Since P_2 is scalar, the simplest choice for P_2 is the unit. Hence, Eq. (25) can be rewritten as follows:

$$\dot{\tilde{\mathbf{X}}}_1 = (\mathbf{A}_{11} - \mathbf{A}_{12}\mathbf{P}_1)\tilde{\mathbf{X}}_1 \tag{26}$$

The matrix $\mathbf{P}_1$ must be determined such that the motion on the sliding surface is stable. After determining $\mathbf{P}_1$, the unknown matrix $\mathbf{P}$ is obtained from Eq. (22).

According to the LQR method, minimizing the performance index J given by Eq. (20) subjected to the constraint of the equations of motion, Eq. (23) results the following solution [21]:

$$\tilde{X}_2 = -\frac{1}{2}Q_{22}^{-1}\left(\mathbf{A}_{12}'\tilde{\mathbf{P}} + 2\mathbf{Q}_{21}\right)\tilde{\mathbf{X}}_1 \tag{27}$$

where $\tilde{\mathbf{P}}$ is a $(2N-1) \times (2N-1)$ matrix and the solution of the following matrix Riccati equation:

$$\tilde{\mathbf{A}}'\tilde{\mathbf{P}} + \tilde{\mathbf{P}}\tilde{\mathbf{A}} - 0.5\tilde{\mathbf{P}}\mathbf{A}_{12}Q_{22}^{-1}\mathbf{A}_{12}'\tilde{\mathbf{P}} = -2\left(\mathbf{Q}_{11} - \mathbf{Q}_{12}\mathbf{Q}_{22}^{-1}\mathbf{Q}_{12}'\right) \tag{28}$$

in which $\tilde{\mathbf{A}} = \mathbf{A}_{11} - \mathbf{A}_{12}Q_{22}^{-1}\mathbf{Q}_{21}$.

Considering $P_2 = 1$, Eq. (27) yeilds $\tilde{X}_2 = -\mathbf{P}_1\tilde{\mathbf{X}}_1$. Comparing this result and Eq. (27), one obtains:

$$\mathbf{P}_1 = 0.5Q_{22}^{-1}(\mathbf{A}_{12}'\tilde{\mathbf{P}} + 2\mathbf{Q}_{21}) \tag{29}$$

Finally, the matrix $\mathbf{P}$ in Eq. (13) is obtained as follows:

$$\mathbf{P} = \begin{bmatrix} \mathbf{P}_1 & \vdots & 1 \end{bmatrix} \tag{30}$$

3.3. Reduction of control force chattering

The control law (i.e. Eq. (18)) which satisfies the sliding condition (Eq. (15)) is discontinuous across the surface $S(t)$, thus leading in practice to control force chattering. In general, chattering is highly undesirable, since it involves extremely high control activity, and furthermore may excite high–frequency dynamics neglected in the course of modeling [22]. In order to attenuate the chattering phenomenon, in this study a hyperbolic tangent function $tanh(\frac{-}{\varphi})$ was used instead of the sign function $sgn(\square)$. φ is a boundary layer. The sign and hyperbolic tangent functions for different values of φ, are shown in Fig. 2. The

smooth performance of hyperbolic tangent function reduces the chattering effect in control law. In this study, the boundary layer is chosen 0.05.
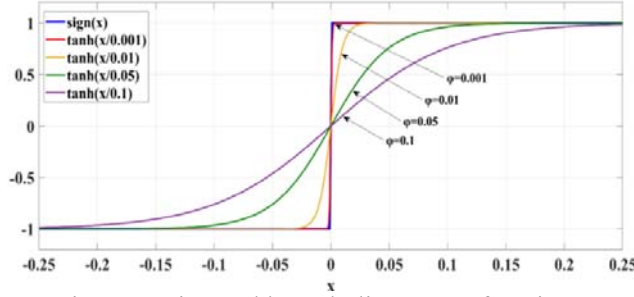

Figure 2. Sign and hyperbolic tangent functions

4. NUMERICAL STURY

4.1. Properties of structure

An 11–story realistic building, located in the city of Rasht, Iran, is considered for the numerical study [12]. By assuming a rigid diaphragm for each of floor levels, a simplified linear model of the realistic building (known as a shear–type building model) is considered as a 2–dimensional shear building. By installing a TMD on the top story, 12 degrees of freedom are adopted to describe the total displacement of the stories of the structure and TMD/ATMD system. The adopted control scheme consists of an ATMD placed on the top floor of the building. From the first to the top floors, the mass of the stories are 215, 201, 201, 200, 201, 201, 201, 203, 203, 203 and 176 tons, respectively. The corresponding stiffness coefficients are 468, 476, 468, 450, 450, 450, 450, 437, 437, 437 and 312 MN/m, respectively. The first and second natural frequencies of the uncontrolled structure are equal to as $\omega_1 = 6.5727$ and $\omega_2 = 19.355$ rad/s, respectively. By assuming the structural damping ratio as the 5% of the critical damping value for the first two modes i.e. $\xi = 0.05$, the damping matrix can be calculated using the Rayleigh damping method in Eq. (5).

4.2. Properties of TMD and ATMD

For the TMD system, the frequency ratio, β_d, is assumed to be the ratio of the natural frequency of the TMD to the first modal frequency of the main structure. In addition, the mass of the TMD is chosen to be α_d–percent of the total mass of the building and the damping ratio of the TMD is considered to be ξ_d–percent of the critical damping value. The optimal values of α_d, ξ_d and β_d were determined by a genetic algorithm in Ref. [12] and were equal to 3%, 7% and 1.0, respectively. For the ATMD system, the optimal values of α_d, ξ_d and β_d are also considered as 3%, 7% and 1.0, respectively.

4.3. Design of sliding surface

In order to design the OSMC technique, the coefficients of the sliding surface are

determined using the LQR method with a diagonal weighting matrix $\mathbf{Q}$. The matrix $\mathbf{Q}$ regulates the penalties on the excursion in the trajectories of the sliding variable (S). Indeed, the random selection of $\mathbf{Q}$ in the OSMC controller can not provide the good set point tracking the performance due to the absence of integral term unlike the PID controller. Therefore, the selection of the matrix $\mathbf{Q}$ has been considered as the key problem in the design of SMC using the LQR method. Conventionally, control engineers often select the weighting matrices based on trial and error procedure, which not only makes the design tedious but also provides a non–optimized response. Hence, there is a need to a systematic approach in the selection the weighting matrix $\mathbf{Q}$.

In the previous studies [12, 16, 17], it was not presented any straightforward procedure for this problem. For overcoming this problem, an approach was to use a simple iteration algorithm for optimizing the elements of matrix $\mathbf{Q}$ [22]. But, this method suggests the way to only choose the initial values of the weighting matrices, and after the first trial the values of the weighting matrices are to be iterated to get the optimal response, which once again leads to manual tuning. Another approach was to select the elements of matrix $\mathbf{Q}$ based on parameters of structure and TMD such as their damping and stiffness. In this study, the matrix $\mathbf{Q}$ was considered as a diagonal matrix and its main diagonal elements were selected as follows:

$$\mathbf{Q} = \begin{bmatrix} \alpha_1 \times k_d & & & & & & & & \\ & \alpha_1 \times k_N & & & & & \mathbf{O}_{(N+1) \times (N+1)} & & \\ & & \ddots & & & & & & \\ & & & \alpha_1 \times k_1 & & & & & \\ & & & & \alpha_2 \times c_d & & & & \\ & & & & & \alpha_2 \times c_N & & & \\ & \mathbf{O}_{(N+1) \times (N+1)} & & & & & \ddots & & \\ & & & & & & & \alpha_2 \times c_1 \end{bmatrix} \quad (31)$$

where c_d is the damping of TMD. $c_i, i = 1, \ldots, N$ presents the damping of $i$the story of structure. α_1 and α_2 are the design parameters.

It is noted that the above form of the matrix $\mathbf{Q}$ represents the sum of the kinetic and damping energies, and it is commonly adopted in structural control applications. In this study, α_1 and α_2 are equal to 0.17 and 0.02, respectively.

4.4. Results of structural control

In order to demonstrate the performance of the OSMC controller in comparison with other control strategies in the literature, the controlled structure with the ATMD system was assessed subjected to two far–fault earthquakes, El Centro (1940) and Hachinohe (1968), as well as two near–fault earthquakes, Northridge (1994) and Kobe (1995). The peak ground acceleration (PGA) of theses earthquakes are equal to 0.83, 0.22, 0.34 and 0.82g [12]. Time–history analyses of the structure are carried out using MATLAB/Simulink software [23].

Tables 1 to 4 compare the maximum displacement of stories for the structure controlled

by the SMC controller subjected to El Centro, Hachinohe, Kobe and Northridge earthquake excitations, respectively. In the tables, the results of the structure controlled by OSMC are also compared with those given by the uncontrolled structure (Unctrl), the structure equipped with TMD (Passive), LQR [12], FLC [12] and PID [24].

Table 1: Comparison of the performance of the different controllers in El Centro earthquake

Story	Maximum responses of stories (m)						Parentage of reduction (%)				
	Unctrl	Passive	LQR [12]	FLC [12]	PID [24]	OSMC	Passive	LQR [12]	FLC [12]	PID [24]	OSMC
1	0.019	0.013	0.009	0.009	0.014	0.008	31.6	52.6	52.6	26.3	57.9
2	0.039	0.025	0.018	0.016	0.028	0.016	35.9	53.8	59.0	28.2	59.0
3	0.057	0.037	0.027	0.023	0.041	0.024	35.1	52.6	59.6	28.1	57.9
4	0.074	0.048	0.035	0.028	0.053	0.032	35.1	52.7	62.2	28.4	56.8
5	0.090	0.058	0.043	0.034	0.064	0.041	35.6	52.2	62.2	28.9	54.4
6	0.100	0.067	0.050	0.039	0.074	0.047	34.4	51.0	61.8	27.5	53.0
7	0.120	0.074	0.058	0.043	0.081	0.053	38.3	51.7	64.2	32.5	55.8
8	0.130	0.083	0.060	0.047	0.087	0.058	36.2	53.9	63.9	33.1	55.4
9	0.140	0.094	0.067	0.049	0.091	0.062	32.9	52.1	65.0	35.0	55.7
10	0.140	0.094	0.070	0.050	0.094	0.064	32.9	50.0	64.3	32.9	54.3
11	0.147	0.099	0.072	0.051	0.096	0.065	32.7	51.0	65.3	34.7	55.8
Average	0.096	0.063	0.046	0.035	0.066	0.043	34.6	52.1	61.8	30.5	56.0

Table 2: Comparison of the performance of the different controllers in Hachinohe earthquake

Story	Maximum responses of stories (m)						Parentage of reduction (%)				
	Unctrl	Passive	LQR [12]	FLC [12]	PID [24]	OSMC	Passive	LQR [12]	FLC [12]	PID [24]	OSMC
1	0.014	0.012	0.011	0.008	0.008	0.011	14.3	21.0	42.9	42.9	21.4
2	0.028	0.024	0.021	0.017	0.015	0.021	14.3	25.0	39.3	46.4	25.0
3	0.040	0.035	0.032	0.024	0.022	0.030	12.5	20.0	40.0	45.0	25.0
4	0.053	0.046	0.041	0.030	0.027	0.039	13.2	22.6	43.4	49.1	26.4
5	0.064	0.055	0.050	0.036	0.031	0.047	14.1	21.9	43.8	51.6	26.6
6	0.074	0.064	0.058	0.040	0.036	0.052	13.5	21.6	45.9	51.4	29.7
7	0.085	0.073	0.065	0.046	0.042	0.057	14.1	23.5	45.9	50.6	32.9
8	0.094	0.081	0.071	0.050	0.047	0.062	13.8	24.5	46.8	50.0	34.0
9	0.100	0.089	0.076	0.053	0.052	0.066	11.0	24.0	47.0	48.0	34.0
10	0.110	0.095	0.079	0.055	0.055	0.068	13.6	28.2	50.0	50.0	38.2
11	0.110	0.099	0.083	0.057	0.058	0.070	10.0	24.5	48.2	47.3	36.4
Average	0.070	0.061	0.053	0.038	0.036	0.048	13.1	23.3	44.8	48.4	30.0

As can be seen from Tables 1 to 4, the OMSC controller reduces the maximum displacement of the top stroy (roof) responses of the structure about 55.8%, 36.4%, 37% and 5.2% in comparison with that of the uncontrolled structure subjected to El Centro, Hachinohe, Kobe and Northridge earthquakes. Therefore, the numerical results demonstrate

that OSMC can significantly control the structure subjected to earthquakes. Similarly, it is obvious from Table 1 to 4, OSMC in comparison with LQR indicates the better performance in the reduction of the seismic responses.

Table 3: Comparison of the performance of the different controllers in Kobe earthquake

Story	Maximum responses of stories (m)						Parentage of reduction (%)				
	Unctrl	Passive	LQR [12]	FLC [12]	PID [24]	OSMC	Passive	LQR [12]	FLC [12]	PID [24]	OSMC
1	0.060	0.049	0.050	0.046	0.050	0.037	18.3	16.7	23.3	16.7	38.3
2	0.120	0.098	0.101	0.092	0.100	0.075	18.3	15.8	23.3	16.7	37.5
3	0.180	0.149	0.144	0.131	0.144	0.113	17.2	20.0	27.2	20.1	37.2
4	0.240	0.199	0.192	0.180	0.191	0.151	17.1	20.0	25.0	20.6	37.1
5	0.290	0.238	0.241	0.229	0.231	0.186	17.9	16.9	21.0	20.3	35.9
6	0.340	0.289	0.269	0.258	0.272	0.219	15.0	20.9	24.1	20.0	35.6
7	0.390	0.332	0.308	0.293	0.306	0.248	14.9	21.0	24.9	21.5	36.4
8	0.430	0.361	0.344	0.335	0.338	0.273	16.0	20.0	22.1	21.5	36.5
9	0.460	0.391	0.363	0.354	0.359	0.293	15.0	21.1	23.0	21.9	36.3
10	0.480	0.408	0.374	0.360	0.375	0.306	15.0	22.1	25.0	21.9	36.3
11	0.500	0.420	0.390	0.370	0.384	0.315	16.0	22.0	26.0	23.1	37.0
Average	0.317	0.267	0.252	0.241	0.250	0.201	16.4	19.7	24.1	20.4	36.7

Table 4: Comparison of the performance of the different controllers in Northridge earthquake

Story	Maximum responses of stories (m)						Parentage of reduction (%)				
	Unctrl	Passive	LQR [12]	FLC [12]	PID [24]	OSMC	Passive	LQR [12]	FLC [12]	PID [24]	OSMC
1	0.046	0.040	0.033	0.031	0.032	0.032	13.0	28.3	32.6	29.6	30.4
2	0.088	0.080	0.063	0.058	0.062	0.059	9.1	28.4	34.1	30.0	33.0
3	0.123	0.109	0.109	0.080	0.087	0.083	11.4	11.4	35.0	28.9	32.5
4	0.150	0.140	0.110	0.099	0.107	0.103	6.7	26.7	34.0	28.7	31.3
5	0.180	0.160	0.130	0.119	0.126	0.119	11.1	27.8	33.9	29.8	33.9
6	0.194	0.178	0.149	0.130	0.143	0.138	8.2	23.2	33.0	26.5	28.9
7	0.204	0.190	0.169	0.139	0.156	0.155	6.9	17.2	31.9	23.8	24.0
8	0.210	0.200	0.181	0.143	0.165	0.169	4.8	13.8	31.9	21.3	19.5
9	0.220	0.220	0.189	0.156	0.168	0.188	0.0	14.1	29.1	23.4	14.5
10	0.230	0.230	0.209	0.168	0.188	0.204	0.0	9.1	27.0	18.3	11.3
11	0.230	0.230	0.219	0.170	0.207	0.218	0.0	4.8	26.1	9.8	5.2
Average	0.170	0.162	0.142	0.118	0.131	0.133	6.5	18.6	31.7	24.6	24.1

In order to compare the performance of TMD (Passive) and ATMD achieved by other control methods, the average of the reductions in the displacement of all stories is depicted in Fig. 3 for different earthquake excitations. Furthermore, the total average of the reductions in the displacement of all stories for TMD and different controllers are displayed in Fig. 3.

It is found from Fig. 3 that ATMD in comparison with TMD can significantly control the the structure for a wide range of earthquakes with various intensities and frequency.It reveals from Fig. 3 that OSMC controller in comparison with the LQR and PID controllers provides the best performance in reducing the maximum displacement of all stroies of the structure. Based on the total average reduction of the maximum displacement for all stroies

shown in Fig. 3, the the total average reduction for the OSMC controller is equal to 36.7%, while this value the LQR and PID controllers are equal to 28.4% and 31%, respectively. It is noted that the total average for the FLC controller is equal to 40.6%, which slightly is better than that of the OSMC controller.
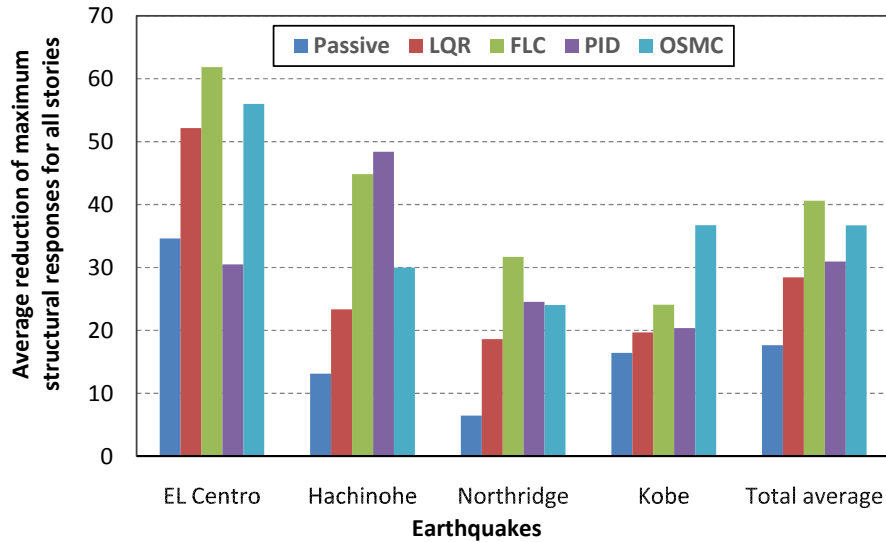

Figure 3. The average reduction of maximum structural responses for all stories

Figs. 4 to 7 show the comparison of the displacement time history of the top story for the structure equipped with TMD and ATMD controlled by the OSMC scheme. As can be seen from Figs. 4 to 7, the OSMC controller efficiently reduces the maximum displacement of the structure subjected to different earthquake excitations.
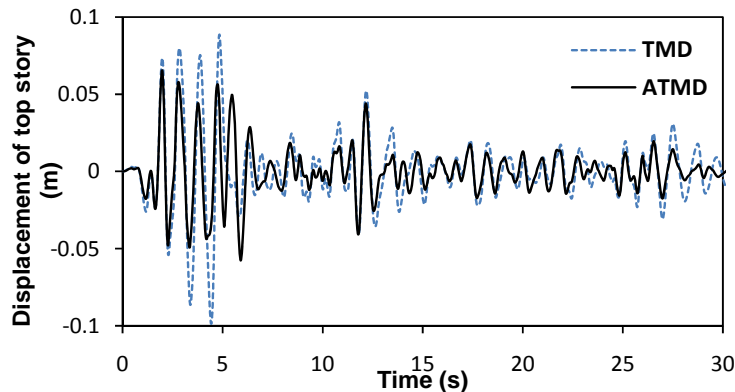
Figure 4. The comparison of the displacement time history of the top story for the structure equipped with TMD and ATMD controlled by OSMC during El Centro earthquake
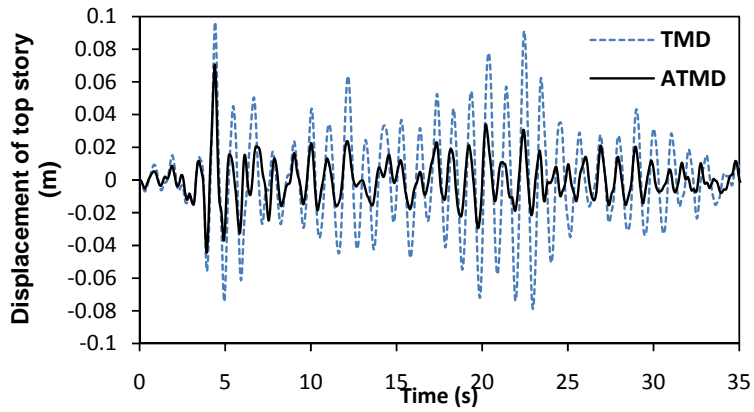
Figure 5. The comparison of the displacement time history of the top story for the structure equipped with TMD and ATMD controlled by OSMC during Hachinohe earthquake
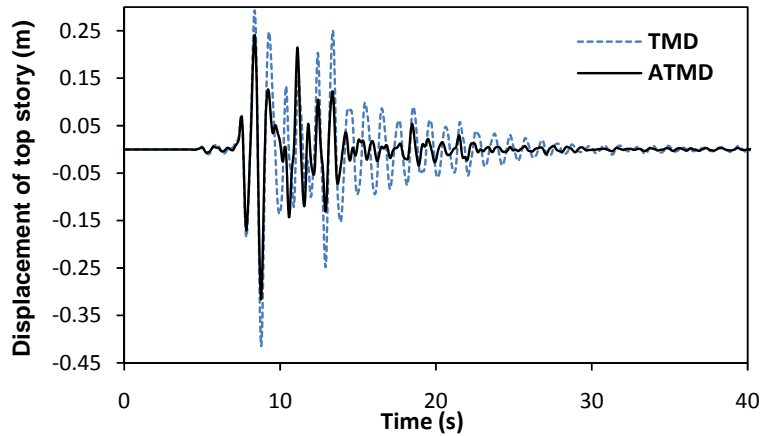
Figure 6. The comparison of the displacement time history of the top story for the structure equipped with TMD and ATMD controlled by OSMC during Kobe earthquake
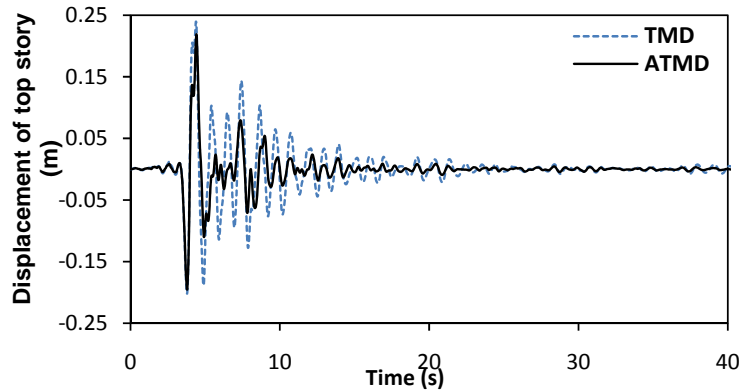

Figure 7. The comparison of the displacement time history of the top story for the structure equipped with TMD and ATMD controlled by OSMC during Northridge earthquake

5. CONCLUSIONS

This paper focused on the development of an optimal sliding mode control (OSMC) for the reduction of the seismic responses of a building subjected to earthquake excitations using the ATMD system. In the OSMC technique, a linear sliding surface, which passed through the origin, was used with the slope of this surface designed such that a given (or desired) cost function was minimized. For the numerical study, an 11–story realistic shear building equppied with a TMD (as a passive system) was considered subjected to different earthquake excitations and the efficiency of the OSMC technique was demonstrated. As well, the performance of OMSC was compared with that of the LQR, FLC and PID contorollers. The numerical results indicated that OSMC was more effective than the passvie controller system (TMD). Furthermore, the total average reduction of the displacements of the building for all studied earthquake excitations was adopted for the comparison of the performance of the controllers. The OSMC controller provided a reduction about 36.7%, while this value for LQR and PID controllers is 28.4% and 31%, respectively. Therefore, the OSMC controller performed better than LQR and PID controllers in the mitigation of the sructural responses. The total average for the FLC controller was also equal to 40.6%, which slightly was better than that of the OSMC controller.

REFERENCES

1. Kaveh A, Mohammadi S, Khadem Hosseini O, Keyhani R, Kalatjari VR. Optimum parameters of tuned mass dampers for seismic applications using charged system search, *IJST, Trans Civil Eng* 2015; **39**, 21-40.
2. Uz ME, Sharafi P, Investigation of the optimal semi–active control strategies of adjacent buildings connected with magnetorheological dampers, *Int J Optim Civil Eng* 2016; **6**(4): 523–47.
3. Etedali S, Mollayi N, Cuckoo search–based least squares support vector machine models for optimum tuning of tuned mass dampers, *Int J Struct Stab Dyn* 2018; **18**(2): 1850028.
4. Sarbjeet S, Datt TK, Open closed loop linear control of building frames under seismic excitation, *J Struct Eng, ASCE* 1998; **124**(1): 43–51.
5. Aldawod M, Samali B, Naghady F, Kwok Kenny CS, Active control of along wind response of tall building using a fuzzy controller, *Eng Struct* 2001; **23**:1512–22.
6. Aldemir U, Evaluation of disturbance weighting parameter of minimax attenuation problems, *Comput Aided Civil Inf Eng* 2009; **24**(4):302–8.
7. Alavinasab A, Moharrami H, Khajepour A, Active control of structures using energy–based LQR method, *Comput Aided Civil Inf Eng* 2006; **21**(8): 605–11.
8. Palazzo B, Petti L, Optimal structural control in the frequency domain: control in norm H_2 and H_∞, *Struct Control Health Monit* 1999; **6**(2): 205–21.
9. Huo L, Song G, Li H, Grigoriadis K, H_∞ robust control design of active structural vibration suppression using an active mass damper, *Smart Mater Struct* 2008; 17(1) 015021 (10pp).

10. Park S, Lee J, Jung H, Jang D, Kim S, Numerical and experimental investigation of control performance of active mass damper system to high–rise building in use, *Wind Struct* 2009; **12**(4): 313–32.
11. Samali B, Al–Dawod M, Performance of a five–storey benchmark model using an active tuned mass damper and a fuzzy controller, *Eng Struct* 2003; **25**(13): 1597–610.
12. Pourzeynali S, Lavasani HH, Modarayi AH, Active control of high rise building structures using fuzzy logic and genetic algorithms, *Eng Struct* 2007; **29**(3): 346–57.
13. Wang P, Lin YH, Vibration control of a tall building subjected to earthquake excitation, *J Sound Vib* 2007; **299**(4): 757–73.
14. Zamani A, Tavakoli S, Etedali S, Control of piezoelectric friction dampers in smart base–isolated structures using self–tuning and adaptive fuzzy proportional–derivative controllers, *J Intell Mater Syst Struct* 2017; **28**(10): 1287–302.
15. Aguirre N, Ikhouane F, Rodellar J, Proportional–plus–integral semi–active control using magnetorheological dampers, *J Sound Vib* 2011; **330**(10): 2185-200.
16. Etedali S, Sohrabi MR, Tavakoli S, Optimal PD/PID control of smart base isolated buildings equipped with piezoelectric friction dampers, *Earthq Eng Eng Vib* 2013; **12**(1): 39–54.
17. Etedali S, Tavakoli S, Sohrabi MR, Design of a decoupled PID controller via MOCS for seismic control of smart structures, *Earthqukes Struct* 2016; **10**(5): 1067–87.
18. Yang JN, Agrawal AK, Samali B, Wu JC, Benchmark problem for response control of wind–excited tall buildings, *J Eng Mech* 2044; **130**(4): 437–46.
19. Adhikari R, Yamaguchi H, Sliding mode control of buildings with ATMD, *Earthq Eng Struct D* 1997; **26**(4): 409–22.
20. Wu JCh, Yang JN, Modified sliding mode control for wind–excited benchmark problem, *J Eng Mech, ASCE* 2004; **130**(4): 449–504.
21. Yang LN, Li Z, Vongchavalitkul S, A generalization of optimal control theory: Linear and nonlinear control, *J Eng Mech*, *ASCE* 1994; **120**(2): 266–83.
22. Bryson AE, Applied optimal control: optimization, estimation and control. Routledge, 2018.
23. MATLAB, *The Math Works*, Inc, Natick, MA, 2000.
24. Etedali S, Zamani A, Tavakoli A. A GBMO–based PI$^{\lambda}$–D$^{\mu}$ controller for vibration mitigation of seismic–excited structures, *Automat Constr* 2018; **87**: 1–12.